Journal of Applied Fluid Mechanics, Vol. 8, No. 1, pp. 33-42, 2015.
Available online at www.jafmonline.net, ISSN 1735-3572, EISSN 1735-3645.
DOI: 10.36884/jafm.8.01.20353

Modeling Open-Flow Steam Reforming of Methanol over $Cu/ZnO/Al_2O_3$ Catalyst in an Axisymmetric Reactor

L.Pacheco[1], D. Della-Valle[1,2], O. Le Corre[3],C. Habchi[4], T. Lemenand[1], H. Peerhossaini[5†]

[1]*LUNAM Université, Laboratoire de Thermocinétique de Nantes, CNRS UMR 6607, 44306 Nantes, France*
[2]*ONIRIS, B.P. 85222 – F-44322, France*
[3]*GEPEA, Ecole des Mines de Nantes, CNRS-UMR 6144, B.P. 20722 – F-44307, France*
[4]*Energy and Thermo-Fluids Group, School of Engineering, Lebanese International University LIU, Beirut, Lebanon*
[5]*Univ. Paris Diderot, Sorbonne Paris Cité, Institut des Energies de Demain (IED), Paris, France*

†*Corresponding Author Email: hassan.peerhossaini@univ-paris-diderot.fr*

(Received May 6, 2013; accepted March 17, 2014)

ABSTRACT

This paper describes a CFD study of the steam-reforming process (SRP) of methanol in a short pseudo-contact time reactor of fixed bed type, in axi-symmetric conditions. The SRP is important sake for hydrogen production, and the design /scale-up/control of the industrial processes in the future are supported by a reliable knowledge and prediction of the catalytic reaction. The difficulty of determining the reaction scheme and the associated constants is well-known, due to the necessity of identifying the reaction kinetics in purely chemical regime, meaning with a perfect homogeneity and flow independence. Practically these ideal conditions, albeit assumed, are not fulfilled so that the intrinsic chemical kinetics is not reached. For the case of SRP, we have attempted here to validate the Peppley's model by a numerical modelling reproducing exactly the local conditions in the experimental duct, accounting for gradients in the cross section. The numerical results show the same trends than the experimental one, but with a slight shift of 20% as a consequence of the reactor heterogeneity. This result seems acceptable to validate the use of the Peepley's model for further studies in other types of complex flow reactors.

Keywords: Methanol; Bio-methanol; Steam reforming; Hydrogen production; Multifunctional heat exchanger.

NOMENCLATURE

C_p	specific heat
C_{si}	active site concentrations of type *i*
D	diameter
d_p	catalytic bead size
E	activation energy
F	molar flow
h	enthalpy
ΔH	adsorption heat
k	kinetic constants
k^{∞}	pre-exponential term in Arrhenius equation
K	adsorption constants
L	reactor length
m_{cat}	catalyst mass
M	molar mass
p	pressure
r	reactor radio
$\dot{r}_i$	rate of reaction or production of species *i*

Subscripts

cat	catalyst
i	chemical species
R	reactor
wall	wall

R	gas constant
S	reaction heat
ΔS	entropy of adsorption
S_p	particle specific surface
S_g	specific surface
T	temperature
u	velocity component in the axial direction
V	velocity component in the radial direction
$\vec{v}$	velocity vector
W	catalysts mass
Y	mass fraction
z	length reactor

Greek letters

λ	thermal conductivity
μ	viscosity
ρ	density
ε	packed bed porosity

Acronym

MD	methanol-decomposition reaction
SRM	steam-reforming reaction
WGS	water-gas shift reaction

1. INTRODUCTION

Restrictions on the use of fossil-based energy sources are ever becoming more stringent. The European Union's 2008 CLIMAT plan aims at a 20% reduction of CO_2 emissions and consumption of primary energy sources, and a 20% increase in energy production from renewable sources. Hydrogen is among the solutions considered in the context of decarbonised electricity production. However, implementing this technology still involves severe socioeconomic and safety-related difficulties. The significant storage problems in using hydrogen for transport applications must be solved before it is accepted as a widely used transportation fuel.

In addition, hydrogen is not a primary energy source but an energy vector: chemical reactions must be used to extract it from hydrocarbons. Hydrogen can be produced from several hydrogen-rich primary fuels such as methanol, natural gas, ethanol or gasoline. These fuels are abundant, especially methane (and hence methanol, since it can be produced from methane). Actually, the electricity produced by fuel cells can be qualified of "green electricity" if the fuel comes from the biomass, to compensate for the carbon budget. Several reactions can be envisaged for hydrogen production from the above primary fuels:

- steam reforming, an endothermic reaction with pure water that produces hydrogen as well as carbon monoxide and carbon dioxide.
- partial oxidation, an exothermic reaction with oxygen that produces hydrogen as well as carbon monoxide.

Table 1 shows the principal characteristics of some hydrogen production processes for several reactants rich in hydrogen. The molar fraction of hydrogen is important for fuel-cell applications since cell efficiency strongly depends on hydrogen purity, so that the partial oxidation reaction shown in table 1 is not recommended for hydrogen production.

Since carbon monoxide is a poison, hydrogen production by methanol steam reforming is more appropriate for this application because its rate of CO production is two orders of magnitude smaller than in the other hydrogen production modes. However, in other processes of hydrogen production, it is necessary to add a gas purification step before the fuel cell with a water-gas shift reaction to transform the carbon monoxide to carbon dioxide. Since this reaction occurs at 473 K, it is necessary to add another reactor for gas purification. This reactor is not needed if methanol steam reforming is used for hydrogen generation.

Table 1 also shows that the methanol steam reforming is the only process in which the reactions occur at moderate temperatures (less than 800 K). Higher reaction temperatures consume more energy and require more expensive materials. In addition, extra safety precautions are needed.

Another advantage of methanol steam reforming is its low sulfur content. In fact, all the processes considered for hydrogen production utilize catalysts. Many catalysts used in the vapor phase are sensitive to impurities. Sulfur is present in most gas fuels and is also a poison, so that it must be removed before being introduced into the hydrogen production process. Since catalysts are used in several stages of methanol production, the sulfur can be removed in early stages, leaving methanol a sulfur-free liquid primary fuel.

Table 1 Characteristics of different processes for hydrogen production

Primary fuel	Hydrogen molar fraction (dry fraction *%mol*)	CO molar fraction in product (*%mol*)	Reaction temperature (*K*)
Steam reforming of :			
Methane	78	11.2	1000 – 1100
Methanol	71.9	0.8	500 – 600
Ethanol	71.5	10 - 14	800 – 1000
Gasoline, gasoil, fuel	73.3	20	1000 – 1150
Partial oxydation of :			
Methane	46.3	20	1500 – 1600
Gasoline, diesel, fuel	34	25	1150 – 1900

For all these reasons, methanol (bio-methanol) is a very advantageous fuel for hydrogen production by chemical conversion. Indeed, the C/H ratio for methanol is 0.25, compared to 0.7 for gasoline, 0.5 for diesel and 0.25 for methane. Furthermore, methanol does not contain carbon-carbon bonds. Methanol steam reforming makes it possible to produce hydrogen with high conversion rates at low temperatures (550-580 K) with less by-product (CO) formation than other fuels.

1.1 Previous catalyst work

The methanol steam reforming process (SRP) has been studied extensively. Previous work has suggested that the SRP can be adequately modeled using the overall reaction: methanol steam reforming (SRM), methanol decomposition (MD) and water-gas shift (WGS), see Dümpelmann and Baiker (1992) Peppley et al. (1992a-b).

Catalyst performance has been studied in terms of both increased CH_3OH conversion and decreased CO production. The steam-reforming process (SRP) of methanol occurs over Cu or Pd/Zn alloy catalysts at low temperatures (200°C to 300°C), see Zhao et al. (2007). These different catalysts have different advantages and drawbacks.

Copper-based catalysts have been widely studied in the SRM reaction. Ranganathan et al. (2005) showed that the most suitable catalyst for SRP is $Cu/ZnO/Al_2O_3$. However, this catalyst is unstable at high temperatures (approximately 300°C) and is very susceptible to thermal sintering via a surface migration process. Copper-based catalysts normally contain oxides that increase stability, mainly by physically separating the copper crystallites. In addition, synergetic effects have

been observed, e.g. alloy formation, morphology changes or the induction of strain in the copper crystalline structure (for Cu over ZnO), see Zhao et al. (2007). The catalyst preparation method affects performance (e.g. CO selectivity, catalyst stability). The copper co-precipitation method is the most commonly used method of catalyst preparation, see Gunter et al. (1995).

Takezawa and Iwasa (1997) studied the SRP and catalytic performance of copper and group VIII metals (Cu, Ni, Rh, Pt and Pd) on SiO_2; higher performance (in selectivity and activity) was obtained by using Cu/SiO_2. Later, using an impregnation catalyst method, Takezawa and Iwasa (1997) and Iwasa et al. (1993) studied the selectivity for the SRP of Pd catalysts on different supports (ZnO, Al_2O_3, SiO_2 Nb_2O_5, Nd_2O_3, La_2O_3 and ZrO_2), concluding that copper-based catalysts and Pd/ZnO offered high performance for SRP. They also noted that Pd/Zn alloys increase the performance of Pd/ZnO catalysts for the SRP and that the Pd/Zn alloys exhibit excellent thermal stability.

Lindström and Pettersson (2001,2002), used copper-based catalysts on an Al_2O_3 support to compare the catalytic activity of promoters Cr, Zn and Zr. They showed that large copper content in the catalyst increases H_2 and CO_2 selectivity except for Cu/Zn, where the activity is almost invariant and the promoter Zn has a greater affinity to CO_2 selectivity and methanol conversion than Cr, Zr promoters. They also showed that the addition of a Zr promoter increases methanol conversion. Lindström and Pettersson (2001) compared the stability of copper-based catalysts Cu/ZrO_2 and a commercial $Cu/ZnO/Al_2O_3$ catalyst, finding that the zirconium- doped catalysts show high CO_2 selectivity but H_2 production is decreased.

Takeguchi et al. (2002) compared copper-based and palladium-based catalysts for SRP at different reaction temperatures with two preparation methods, impregnation and co-precipitation. Experimental tests showed that copper-based catalysts over ZnO/Al_2O_3 have the greatest H_2 production rate (highest methanol conversion) and high CO_2 selectivity, see Agrell (2003), Guichard (2007), Purnama et al. (2004a), Zhao et al. (2007). Figure 1 compares the different catalysts for H_2 production rate as a function of temperature.

1.2 Kinetic mechanisms in methanol steam reforming

Kinetic mechanisms in methanol-steam reforming on $Cu/ZnO/Al_2O_3$ have also been studied extensively. Jiang et al. (1993a-b) used a U-tube reactor (I.D. 6 mm) maintained at atmospheric pressure and constant temperature. They developed a reaction mechanism in SRM by regression analysis of methanol synthesis in which the adsorption of CH_3OH and H_2 significantly affects the reaction rate; CO_2 has no effect. They suggested a process that is 100% selective for CO_2 in which the rates of WGS and MD reactions are negligible, and concluded that CO_2 has no influence on the reaction rates and affirmed that the SRP is 100% selective for CO_2 and H_2 and that CO is not detected for temperatures lower than 533 K. Further, they suggested

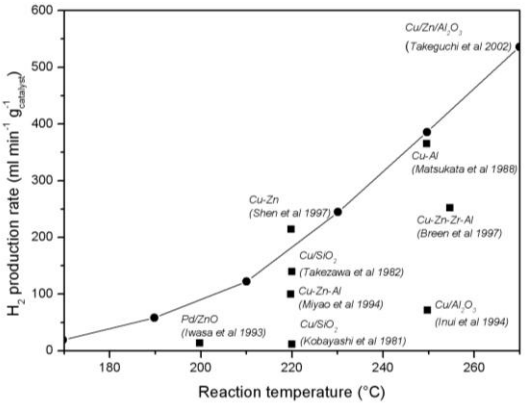

Fig. 1. Comparison of catalytic performance for SRM reactions: (●) impregnation catalyst; (■) co-precipitation catalyst, see Lindstrom and Pettersson (2001-b)

that CO is not the intermediate product of the SRP process over copper-based catalysts. They found that water-gas shift reaction takes place under the operational conditions of the SRP. Their infrared studies showed that competitive adsorption takes place between CH_3OH and CO by which the CH_3OH is preferentially adsorbed.

Agrell et al. (2002) used a tubular quartz reactor (I.D. 6 mm) at atmospheric pressure with helium as the carrier gas. They assumed isothermal reaction conditions and negligible transfer resistance. Agrell (2003) neglected the MD reaction and attributed CO formation to a reversible WGS reaction. He suggested that the CO is a secondary product formed at higher temperatures by a reversible WGS reaction and confirmed that the WGS reaction is favored by a lower pseudo-contact time and a higher temperature. Jiang et al. (1993a-b) had also developed a model to predict the rates of formation of CO_2 and H_2, but this model did not predict CO formation; they showed CO formation experimentally at low temperatures.

The model proposed by Purnama et al. (2004b), on the other hand, predicted CO formation and showed that it can be influenced by catalyst particle size. They used a tubular stainless steel reactor (I.D. 10 mm) at atmospheric pressure and isothermal conditions to study the catalytic activity and selectivity of Cu/ZrO_2 and commercial $CuO/ZnO/Al_2O_3$ in long-duration tests and showed that methanol conversion is more favored by $CuO/ZnO/Al_2O_3$ catalyst. Agrell et al. (2002) and Purnama et al. (2004b) reported negligible CO production by the reversible WGS reaction and MD reaction. Table 2 shows their different experimental conditions. The density considered is 1100 $kg.m^{-3}$ and the porosity calculated for body-centered cubic packing is 0.32.

Several different kinetic mechanisms have been proposed for SRP, see Jiang et al (1993a-b), Peppley et al. (1992a-b), Purnama et al. (2004b). Dümpelmann and Baiker (1992) measured the SRM and MD reaction rates under various operating conditions that maintained the WGS reaction in equilibrium, adjusting the partial pressure of CO. Under these conditions, they concluded

Table 2 Experimental conditions in litterature

	Jiang et al. 1993	Peppley et al. 1999	Agrell 2003	Purnama et al. 2004
Catalyst $Cu/ZnO/AL_2O_3$	BASF S3-85	BASF K3-110	G-66 MR	Süd-chimie 50 % Cu
$S_g\ [m^2.kg^{-1}]$	83 x 10^3	102 x 10^3	70 x 10^3	70 x 10^3
$W_{cat}\ [kg]$	0.5 x 10^{-3}	77 x 10^{-6}	50 x 10^{-6}	200 x 10^{-6}
$d_p\ [mm]$	0.36	1	0.25	0.71
$D_R\ [mm]$	6	22.1	6	10
$T_{wall}\ [K]$	513	553	533	523
$P\ [bar]$	1	1.16	1	1
H_2O/CH_3OH	1	1.36	1.3	1
$N_2\ [m^3min^{-1}]$	-	-	0.2 x 10^{-3}	-

that methanol is converted principally to CO_2 and that the MD reaction produces a negligible amount of CO. They suggested that the MD reaction rate is lower than that of the WGS reaction.

1.2 Objective of the study

Peppley et al. (1992a-b) proposed one of the most reliable and comprehensible reaction networks for modeling SRP in which SRM, MD and WGS reactions are included. This model shows that there is one type of catalyst site for the MD reaction and another type for the SRM and WGS reactions. Experiments by Peppley et al. (1992a-b) confirmed the results in Dümpelmann and Baiker (1992), Jiang et al. (1993a-b).

Here we develop Peppley's et al. (1992a-b) reaction mechanism using numerical integration of a plug-flow tubular reactor model, assuming isothermal wall conditions and a pure methanol-steam feed. In Peppley's et al. (1992a-b) model, these kinetic mechanisms were developed by measuring the CH_3OH conversion percentage at the reactor entrance and exit (which was assumed isothermal). Thus the temperature gradients in the reaction zone and the effect of reactant flow on the reactions were not considered. In this work we take these effects into consideration and show that they affect the conversion rates of the different species.

The kinetic mechanism proposed by Peppley et al. (1992a-b) present the advantage of predicting CO formation, which is not generally taken into account. The numerical simulations presented here were performed to reproduce Peppley's experiments in a fixed-bed reactor made up of spherical beads coated with catalyst. Comparison between simulation and experimental results opens the discussion of the chemical model. The model can also be used to explore favourable conditions for high CH_3OH conversion rates and low by-product formation

2. MATHEMATICAL AND NUMERICAL MODELS

2.1 Conservation equations

The conservation equations are solved for laminar flow, ignoring gravitational external body forces. In order to describe the complex reforming process in a computer model, a number of assumptions on the physical conditions are made:

1. the fixed-bed (bead-bed) catalyst is modelled by a porous medium and treated as a pseudo-homogeneous medium with given homogenized physical properties
2. flow is axisymmetric, laminar and steady
3. bed porosity is constant in axial and radial directions (isotropic)
4. gases are assumed incompressible
5. the chemical reaction occurs only at the bead surface
6. catalyst deactivation is neglected
7. heating effect of viscous dissipation is neglected
8. reactor wall and fixed bed temperature are assumed constant
9. physical properties are thermo-dependent
10.

The physical model consists of the following set of equations, for mass, momentum and energy balance:

– continuity equation:

$$\nabla(\rho\,\vec{v}) = 0 \tag{1}$$

– pressure losses:

$$\frac{\Delta p}{L} = \frac{150(1-\varepsilon)}{\varepsilon^3 d_p^2}\mu u + \frac{3.5(1-\varepsilon)}{\varepsilon^3 d_p}u^2 \tag{2}$$

– energy equation:

$$\nabla(\rho\,\vec{v}\,h) = \nabla(\lambda\,\nabla T) + S \tag{3}$$

where S is the reaction heat:

$$S = -\sum_i \left(\frac{h_i^o}{M_i} + \int C_{p,i}dT\right)\dot{r}_i \tag{4}$$

with ρ the density, $\vec{v}$ the velocity vector, p the pressure, μ the viscosity, ε the porosity of the catalytic bed, L the reactor length, h the enthalpy, T the temperature, λ the thermal conductivity, h_i^o the standard formation enthalpy of species i, Y_i the mass fraction of species i, and $\dot{r}_i$ the rate of production or consumption of species i.

The specific enthalpy is defined as:

$$h = \sum Y_i h_i + \frac{p}{\rho} \quad \text{with} \quad h_i = \int_{Tref}^{T} c_{p,i}dT \tag{5}$$

where T_{ref} is the reference temperature and $C_{p,i}$ is the specific heat at constant pressure.

2.2 Chemical model

The rate of production or consumption of each species $\dot{r}_i$ is computed using Peppley's reaction mechanism (Peppley et al. 1992a-b), which can be reduced to a set of three chemical reactions describing the SRP of methanol. The rate of conversion SR and the *CO* formation are predicted by the water-gas-shift (WGS) and methanol decomposition reactions (MD). These reactions are presented in the following, associated with their relative progress rate:

Methanol steam reaction (SRM):

$$CH_3OH + H_2O \Leftrightarrow CO_2 + 3H_2 \tag{6}$$

$$\dot{r}_{SR} = \frac{k_{SR} K_{CH3O(1)} \left(p_{CH3OH} - \frac{p_{H2}^2 p_{CO2}}{k_{SR}\, p_{H2O}} \right) C_{S1} C_{S1a} S_g}{DEN \left(1 + K_{H(1)}^{0.5} p_{H2}^{0.5}\right)} \tag{7}$$

with:

$$DEN = p_{H2}^{0.5} + K_{CH3O(1)} p_{CH3OH} + K_{HCOO} p_{CO2} p_{H2} + K_{OH(1)} p_{H2O}$$

Methanol decomposition reaction (MD):

$$CH_{3OH} \Leftrightarrow CO + 2H_2 \tag{8}$$

$$\dot{r}_{MD} = \frac{k_{MD} K_{CH3O(2)} \left(p_{CH3OH} - \frac{p_{H2}^2 p_{CO}}{k_{MD}} \right) C_{S2} C_{S2a} S_g}{\left(p_{H2}^{0.5} + K_{CH3O(2)} p_{CH3OH} + K_{OH(2)} p_{H2O}\right)\left(1 + K_{H(2)}^{0.5} p_{H2}^{0.5}\right)} \tag{9}$$

Water gas shift reaction (WGS):

$$CO + H_2O \Leftrightarrow CO_2 + H_2 \tag{10}$$

$$\dot{r}_{WGS} = \frac{k_{WGS} K_{OH(1)} p_{H2}^{0.5} \left(p_{CO} p_{H2O} - \frac{p_{H2} p_{CO2}}{K_{WGS}} \right) C_{S1}^2 S_g}{DEN^2} \tag{11}$$

where the kinetic constants are calculated with the Arrhenius law:

$$k_i = k_i^{\infty} \exp\left(E_i / R\,T\right) \tag{12}$$

and the adsorption constants are calculated with the Vant'Hoff's law:

$$K_i = \exp\left(\Delta S_i / R - \Delta H_i / \left(R\,T\right)\right) \tag{13}$$

In practice, we can consider that the reactions take place at the surface of the catalyst particles. In pseudo-homogeneous porous media, this feature is taken into account by a specific surface (S_g) coated with the catalyst and active site concentrations (C_{si}, C_{sia}) in the reaction rates, eqs. (7), (9), (11). The parameters of the kinetic rate expression for methanol steam reforming (SRM), methanol decomposition (MD) and water gas shift (WGS) reactions are given in table 3.

The methanol conversion is based on the carbon balance, see Peppley et al. (1992a-b):

$$\%conv = \left(1 - \frac{F_{CH3OH}}{F_{CH3OH} + F_{CO2} + F_{CO}}\right) * 100 \frac{1}{2} \tag{14}$$

Table 3 Kinetic constants for steam reforming of methanol, Peppley et al. (1992a-b)

Equilibrium constants	k_i^{∞} [$mol.m^2.s^{-1}$] or ΔS_i [$J.mol^{-1}.K^{-1}$]	E_i or ΔH_i [$kJ.mol^{-1}$]
k_{SR}	7.4 x 10^{14}	102.8
k_{WGS}	5.9 x 10^{13}	87.6
k_{MD}	3.8 x 10^{20}	170
K_{CH3O}	-41.8	-20
K_{HCOO}	179	100
K_{OH}	-44.5	-20
K_H	-100.8	-50
$K_{CH3O(2)}$	30	-20
$K_{OH(2)}$	30	-20
$K_{H(2)}$	-46.2	-50
$C_{s1} = C_{s2}$	7.5 x 10^{-6} [$mol.m^{-2}$]	
$C_{s1a} = C_{s2a}$	1.5 x 10^{-5} [$mol.m^{-2}$]	

2.3 Boundary conditions

At the reactor inlet (z = *0*), the flow is assumed homogeneous in temperature, composition, and velocity, with no radial velocity. At the reactor exit (z = 140 mm), pressure is assumed to be the ambient pressure. The wall temperature is fixed by Dirichlet temperature condition, while in the core, a heat flux is assumed between the beads and the gas mixture. This flux is conventionally given by a Nusselt number, taken here equal to 2 for isolate sphere diffusion mode, and a film temperature which is the average between the bead and the gas temperatures. The stability in time of the bead temperature is ensured by the value of the Biot number, which is here about 0.08, enough below the usual critical value of 0.1. This implies that the beads are heated more "rapidly" by the wall, than cooled by the gases.

2.4 Simulation conditions

Simulations are carried out for the conditions of Peppley's experiments in the porous bead bed geometry as shown in figure 2. The experimental tubular reactor studied by Peppley et al. (1992a-b) is preceded and followed by non-catalytic porous media, each 50 mm long to avoid end effects. The catalytic zone of the reactor is 40 mm long, and its diameter is 22.1 mm. The three zones are modelled. The reaction zone contains 0.077 g of catalyst.

The porosity of the body-centered cubic packing is assumed constant at the nominal value of 0.32. Nevertheless, the latter value is not reported in Peppley's study, so that we have to carry out a sensitivity study on this parameter. Geometry, catalyst properties, physical properties and operating conditions are summarized in tables 2 and 4.

Table 4 Physical properties of copper-based catalyst

ρ_{cat} $[kg_{cat}.m^{-3}]$	1100
ε	0.32
λ_{cat} $[W.m^{-2}.K^{-1}]$	0.3
C_{pcat} $[J.kg^{-1}.K^{-1}]$	550

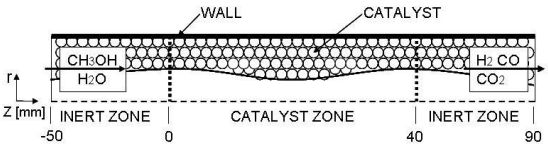

Fig. 2. Tubular reactor model for a constant-porosity fixed catalytic bed

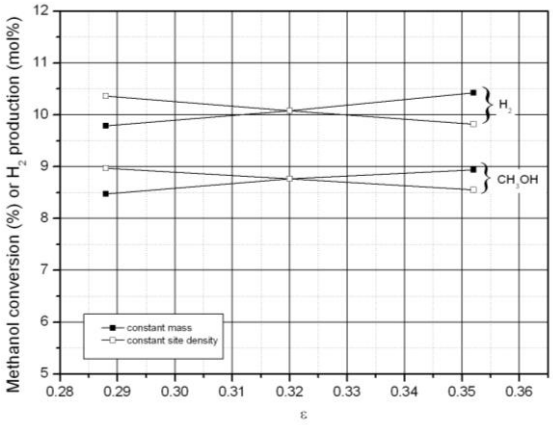

Fig. 3. Porosity sensibility for the methanol conversion (%) and hydrogen production (%)

2.5 Numerical method

The numerical simulations were carried out using the computational fluid dynamics code Fluent (Fluent™, 2001, website), coupled with external subroutines (user-defined functions, UDFs) developed in C++ to implement Peppley's chemical model. A segregated solver, second-order upwind discretization scheme with steady and implicit linearization was used, see Patankar (1980). Pressure-velocity coupling is achieved by the SIMPLE algorithm.

The grid independence was examined in preliminary test runs, with the operating conditions given by Peppley et al. (1992a-b), as presented in table 2. The mesh size effect was evaluated for the methanol steam reforming reactor at a temperature of 553 K, with number of grid cells 75600, 84000 and 94700. The fraction mole deviations of CH_3OH and H_2 for grids 75600 and 84000 are 5% and 26%, and for the grids 84000 and 94700 are 0.4% and 1.9% respectively, as presented in table 5. In the present study a grid of 84000 cells was chosen for the simulation. To determine an adequate convergence criterion, a series of flow simulations were carried out for stop-criterion values ranging from 10^{-3} to 10^{-9}. Beyond the value of 10^{-6}, no significant changes were observed in the velocity field, temperature gradients and reactions rates, and thus 10^{-6} is used as the convergence criterion for all simulations.

3. RESULTS AND DISCUSSION

3.1 Sensitivity of the porosity

In Peppley et al. (1992a-b), the bed catalyst porosity is not reported, and it was hence necessary to validate the choice of a reference value of 0.32 (body-centered cubic packing). As the catalyst specific surface is varying with the porosity in the reactor, two assumptions were made for this test the porosity parameter:

- the catalyst mass is kept constant (variable site active density)
- the active site density is considered constant (variable catalyst mass)

Table 6 Catalytic mass and particle specific surface for different porosity values

ε	m_{cat} [g]	S_p $[m^{-1}]$
0.288	0.080623	4204.72
0.32	0.077	4015.75
0.352	0.073376	3826.77

The specific site active density is function of the catalyst mass distributed on the surface formed by the bed particles, eqs 15 and 16.

$$\rho_{cat-specif} = \frac{m_{cat}}{S_p} \tag{15}$$

where the particle specific surface (S_p) is defined as:

$$S_p = \frac{6(1-\varepsilon)}{d_p} \tag{16}$$

The nominal operation conditions are taken, meaning W/F_{CH3OH} = 6.6641 kg.s.mol^{-1} and the wall temperature at 553 K. The porosity is varied in the range [0.288, 0.352] corresponding to ±10% of the reference value.

The figure 3 shows that the global CH_3OH conversion (%) and H_2 production (% mol) sensitivity is low in our case to porosity parameter, less that 3% and 0.01% for CH_3OH conversion and H_2 production respectively. The table 6 shows the correspondent values of the catalytic mass and particle specific surface for different porosity values.

3.2 Model trends: spatial evolutions

Figure 4 shows the reaction rate profiles for SRM, MD, and WGS reaction rates at different z-axis locations. In the entrance to the catalytic zone ($0 < z < 40$ mm) we observe, as far as the methanol concentration is maximum, a high reaction rate for MD (fig 4b), which is responsible for CO production. Further downstream in the catalytic zone, as CH_3OH conversion becomes significant, the partial pressure of the products (H_2, CO_2

Table 5 Mol fraction of CH_3OH and H_2 for the various grid tests at different z-axis locations

	0	10	20	30	40	50
grid numbers 1E+3	0	10	20	30	40	50
75600	0.422	0.407	0.396	0.386	0.377	0.377
84000	0.421	0.4	0.384	0.369	0.357	0.357
94700	0.421	0.399	0.383	0.368	0.356	0.356
H_2 mole fraction						
75600	0.003	0.026	0.044	0.06	0.073	0.073
84000	0.004	0.037	0.063	0.086	0.105	0.105
94700	0.004	0.038	0.065	0.088	0.107	0.107

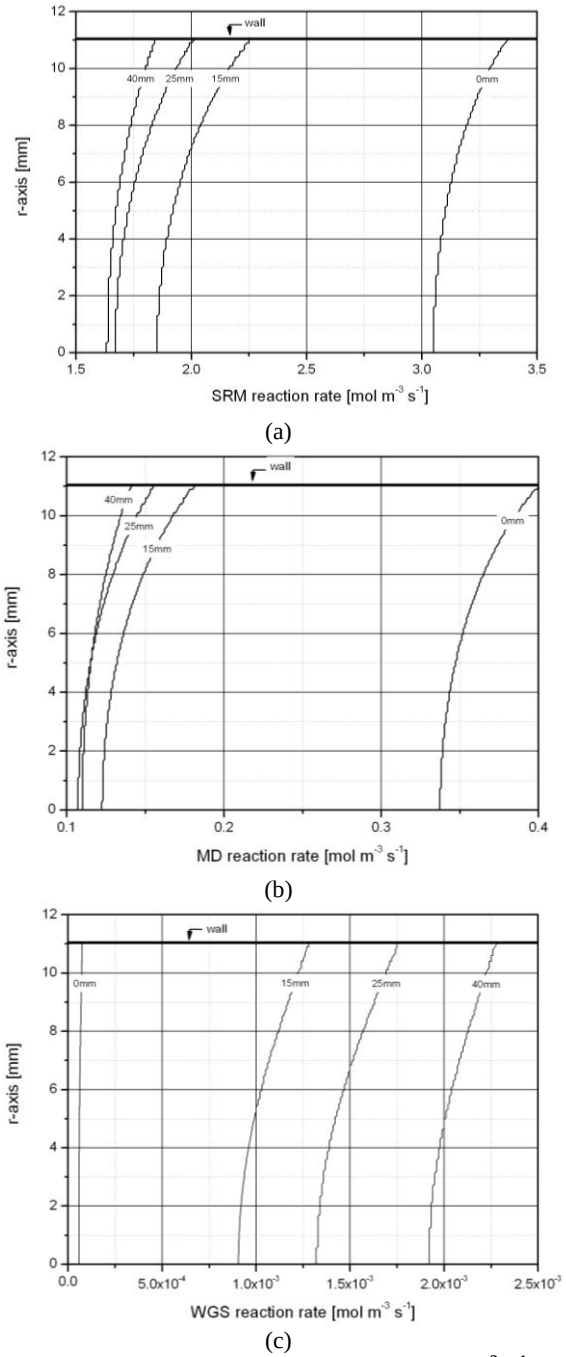

Fig. 4. Profile plots of rate of reaction (kmol.m^{-3}.s^{-1}) at different z-axis locations. H_2O/CH_3OH ratio of 1.36; CH_3OH molar feed rate is 1.16.10^{-4} mol.s^{-1}

and CO) increases and thus the MD reaction rate dramatically decreases (fig 4b), a trend that is even stronger for SRM (fig 4a). However, the combined effect of these two reductions is to increase the cumulative amount of CO produced in the catalytic part of the reactor, as is shown in figure 5d. This observation is in agreement with the experimental results in Dümpelmann and Baiker (1992) and Choi and Stenger (2002). Since CO is principally produced from the MD reaction, its rate of production is also strong in this zone. However, it should be recalled that the CO selectivity is only 2%.

Figure 4c also shows that the WGS is weak at the beginning of the catalytic zone and reaches its maximum at the end of this zone (long contact time). This is due to the fact that at the beginning of the catalytic zone the methanol concentration is high and therefore its rate of absorption by the catalyst is also high. However, further downstream the CO concentration increases while the methanol concentration decreases (fig 5a and 5d) and thus CO absorption by the catalyst is large enough to favour the WGS reaction.

Comparison of figures 4c and 5a shows that high WGS rate takes place where the CH_3OH concentration is low since the conditions are favourable for CO absorption.

Figures 4b and 4c show also that the rates of WGS and MD reactions are stronger near the reactor walls (r = 11.05 mm), where the temperature is high due to the wall heating. This observation (which was in fact expected) shows the importance of taking thermo-fluid-dynamic effects into account in the reaction simulations.

Figure 6 shows that the pressure losses are approximately 2 kPa, less than 2% of the ambient pressure, justifying the assumption of isobaric conditions.

3.3 Model trends: conversion rate

Numerical results on the rate of CH_3OH conversion as a function of pseudo-contact time W/F_{CH3OH} (catalyst mass over CH_3OH molar flow ratio) are plotted in figure 7. Figure 8 shows the rate of CH_3OH conversion as a function of W/F_{CH3OH} for two different wall temperatures (533 K and 513 K), a H_2O/CH_3OH ratio of 1, at 1 bar process pressure. Again, the experimental and numerical results follow the same trends, but the

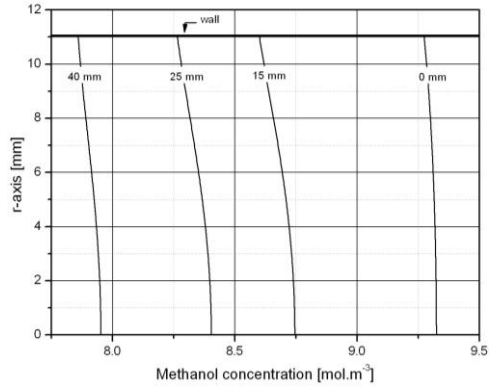

(a)

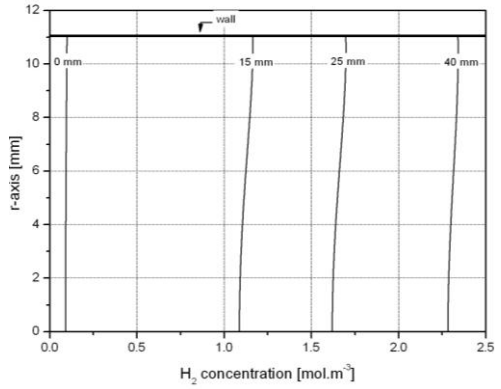

(b)

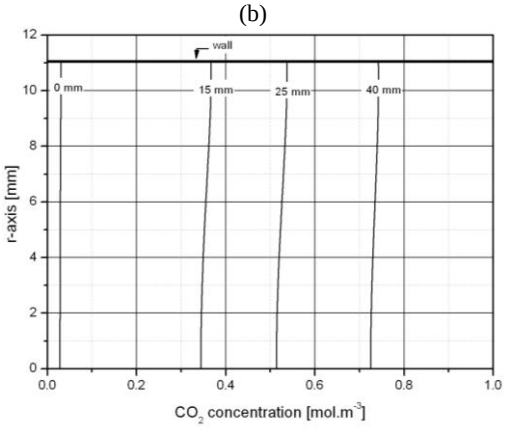

(c)

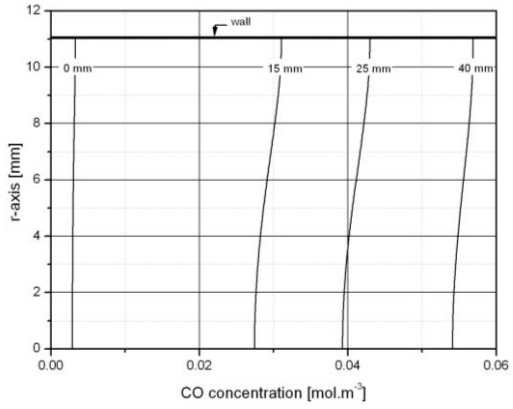

(d)

Fig. 5. Profile plots of the molar concentration for selected species (kmol.m^{-3}), H_2O/CH_3OH ratio of 1.36; CH_3OH molar feed rate is 1.16.10^{-4} mol.s^{-1}

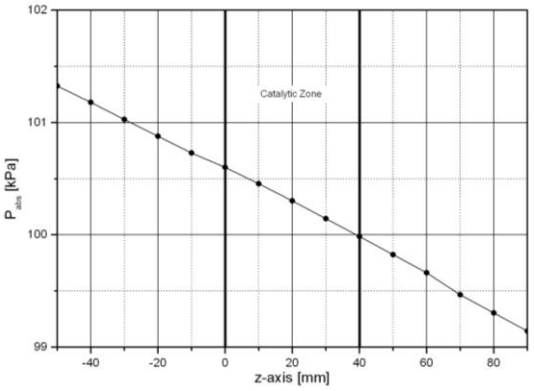

Fig. 6. Profile plots of absolute pressure (kPa), H_2O/CH_3OH ratio of 1.36; CH_3OH molar feed rate is 1.16.10^{-4} mol.s^{-1}.

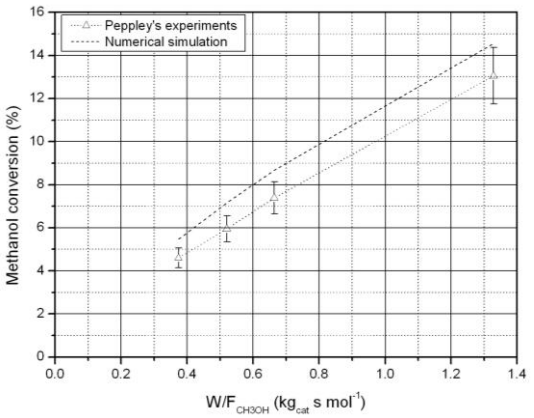

Fig. 7. Methanol conversion as a function of pseudo-contact time W/F_{CH3OH} for Peppley et al. (1992a-b) experiments and present numerical predictions. T_{wall} 553 K, H_2O/CH_3OH ratio of 1.36, 1.16 bar

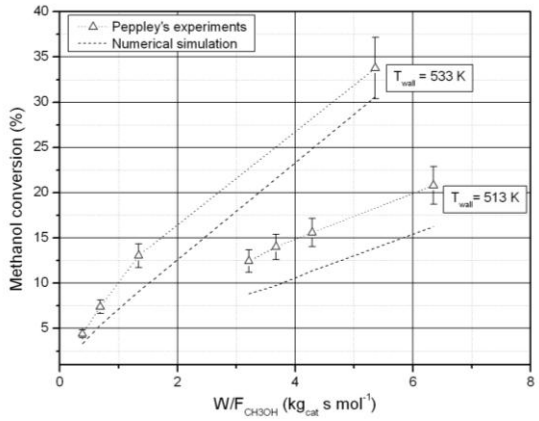

Fig. 8. Methanol conversion as a function of pseudo-contact time W/F_{CH3OH} for Peppley et al. (1992a-b) experiments and present numerical predictions. T_{wall} 533 K, 513 K, H_2O/CH_3OH ratio of 1, 1 bar

absolute values for the methanol conversion rate are slightly different. Figure 8 also show that for a given contact time, the higher the reactor temperature the higher the conversion rate.

Both figures 7 and 8 show that increasing W/F_{CH3OH} is advantageous for methanol conversion. At the same

time, it is shown in Agrell et al. (2002, 2003) that the reversible WGS reactions are also favoured by the increase in W/F_{CH3OH} and consequently there is an increase in CO production. Other parameters also can affect the rate of methanol conversion: the addition of water in the initial gas mixture increases the SRM reaction rate and decreases that of the MD reaction, leading to a reduction in CO production. However, it should be noticed that the addition of water increases the flow rate in the reactor and hence decreases the contact (residence) time. Nevertheless, the global decrease in methanol conversion due to these two opposite effects is less than 5%. The overall effect is that the water addition decreases CO formation, a positive result for hydrogen production aimed at fuel-cell applications. Moreover, extra water is favourable for catalytic activity and decreases catalytic deactivation see Amphlett et al. (1994), Jiang et al. (1993a-b).

3.4 Comparison with the experimental results and discussion of chemical model

The figure 7 compares experimental data from Peppley et al. (1992a-b) with the present numerical predictions for reactor wall temperature 553 K, H_2O/CH_3OH ratio 1.36 and process pressure 1.16 bar. This figure shows that the numerical results follow the same trend as Peppley's experimental results, but with a smaller predicted methanol conversion rates than in the experimental results. The main feature is that the discrepancy can be attributed to the difference between the real local temperature and the global one used in Peppley's computation, since the temperature is the most influential parameter in CH_3OH conversion, see Amphlett et al. (1994). Figure 9 shows the Δ-temperature (ΔT) curve along the catalytic part of the reactor. Peppley et al. (1992a-b) took the reaction temperature as equal to the temperature 1 cm upstream of the entrance to the catalytic bed. This assumption was justified by the fact that in his experiments the temperature difference between the reactor wall and the center (upstream of the entrance to the catalytic zone) was less than 1 K; he thus assumed isothermal conditions and no radial temperature and concentration gradients even in the catalytic zone. However, as figure 9 shows, the temperature difference between the wall and the center of reactor in the catalytic zone is around 6 K, contradicting the isothermal assumption. The high ΔT zone in the middle of the catalytic duct figure 9 shows that the SRP endothermic reaction significantly lowers the temperature.

The table 7 shows the sensitivity of kinetic and adsorption rates basing on the maximal temperature difference in the cross section ΔT, at the reference temperature of 553 K. As is shown in equations (7), (9) and (11), the partial pressures also affect the adsorption constants their influence over the rate is not directly proportional. The kinetic constants k_{SR}, k_{MD} and k_{WGS} present a relative variation of 22%, 19% and 33% respectively from the maximal ΔT. This variation introduces a 10-20% bias (systematic error) in the results, as shown in figures 7 and 8. The kinetic constants are established by Peppley et al (1992a-b) by inverse method assuming a homogeneous temperature

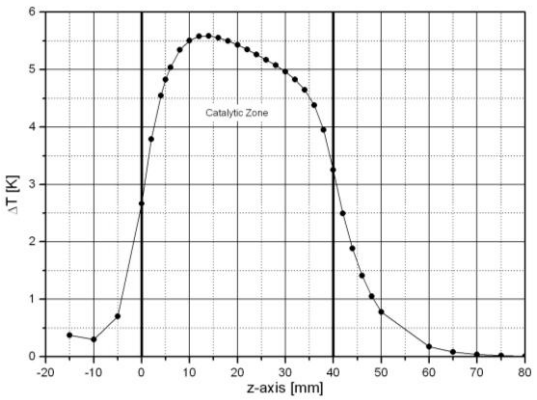

Fig. 9. The Δ-temperature between the catalyst bed and the furnace wall, H_2O/CH_3OH ratio of 1.36; CH_3OH molar feed rate is $1.16.10^{-4}$ mol.s^{-1}

in the reactor, so this assumption leads to a problem of accuracy. Here we show that approximately 1% of temperature gradient gives a 10-20% discrepancy on the conversion rates, what can quantitatively explain the significant deviation between the numerical results and the experiments. Nevertheless, the numerical predictions present consistent trend with the experimental results, justifying the implementation of this kinetic model in the study of SRP intensification.

4. CONCLUSION

In this work, Peppley's mechanism (1992a-b) has been used in a numerical model for predicting the rate of methanol conversion as a function of pseudo-contact time. An external subroutine was developed in Fluent to implement the reaction model. The numerical model allowed prediction of the conversion rate and selectivity, coupled with the pressure and temperature distributions along the catalytic zone of a tubular reactor.

The model permits a better understanding of the local processes, by the identification of production (MD) and consumption (WGS) zones of CO by-products; the MD and WGS reactions are accelerated in high-temperature regions next to the wall. The MD reaction occurs more quickly with a short pseudo contact-time, unlike the WGS reaction, which occurs more quickly for high contact times. This feature is explained by adsorption competition between CH_3OH and CO.

The numerical results show that the temperature distribution is highly non-uniform in the catalytic zone, thus ruling out the assumption of an isothermal reaction. Actually for numerous chemical reactions, temperature is a key parameter in the SRP. We have demonstrated that the assumption of full homogeneity in the Peppley's model gives a 20% shift in the methanol conversion when used in the fixed-bed model. Depending on the final purpose, either the numerical simulation can be used to improve the accuracy of the pre-factors in Peppley's model, or these results can be considered as a satisfactory representation of the intrinsic reaction system to be used in the reacting flow modelling for methanol steam reforming.

ACKNOWLEDGEMENT

The authors would like to thank Dr. Pascal Fongarland and Dr. Dominique Tarlet for contributing ideas. LP would like to acknowledge the financial support of the Conseil Regional des Pays de la Loire.

REFERENCES

Agrell J., H. Birgersson, M. Boutonnet (2002), Steam reforming of methanol over a Cu/ZnO/Al2O3 catalyst: a kinetic and strategies for suppression of CO formation, *J. of Power Sources* 106, 249-257.

Agrell J. (2003), *Development of methanol-reforming catalysts for fuel cell vehicles.* PhD thesis, Royal Institute of Technology, Stockholm.

Amphlett J.C., K.A.M. Creber, J.M. Davis, R.F. Mann, B.A. Peppley, D.M. Stokes (1994), Hydrogen production by steam reforming of methanol for polymer electrolyte fuel cells, *Int. J. of Hydrogen Energy* 19, 131-137.

Choi Y. and H.G. Stenger (2002), Fuel cell hydrogen from methanol on a commercial Cu/ZnO/ AL2O3, *Appl. Catal. B: Environ.* 38, 259-269.

Dümpelmann R. and A. Baiker (1992), Criteria for gradientless operation of internal recycle reactors, *Chem. Eng. Sci.* 47,2665-2670.

Fluent 6.3.26, Copyright Fluent Incorporated, Lebanon, NH, 2001, http://www.fluent.

Guichard A. (2007), *Étude expérimentale et modélisation d'échangeurs compacts multifonctionnels en réaction catalytique.* PhD thesis, Institute National Polytechnique de Toulouse 2007.

Gunter M., T. Ressler, R.E. Jentoft, B. Bems (1995) Redox behaviour of copper oxide/zinc oxide catalyst in the steam reforming of methanol studied by in situ x-ray diffraction and absorption spectroscopy, *J. of Catal.* 203, 133-149.

Iwasa N., S. Kudo, H. Takahashi, S. Masuda (1993), Highly selective supported Pd catalysts for steam reforming of methanol, *Catal. Lett.* 19,211-216.

Jiang C.J., D.L. Trimm, M.S. Wainwright (1993a), Kinetic study of steam reforming of methanol over copper-based catalysts, *Appl. Catal. A: Gen.* 93,245-255.

Jiang C.J., D.L. Trimm, M.S. Wainwright (1993b), Kinetic mechanism for the reaction between methanol and water over a Cu/ZnO/Al2O3, Appl. Catal. A: Gen. 97,145-158.

Karim A., J. Bravo, A. Datye (2005), Nonisothermality in packed-bed reactors for steam reforming of methanol, *Appl. Catal. A: Gen.* 282,101-109.

Lindström B. and L. Pettersson (2001), Hydrogen generation by steam reforming of methanol over copper-based catalyst for fuel cell applications, *Int. J. of Hydrogen Energy* 26,923-933.

Lindström B. and L. Pettersson (2002), Steam reforming of methanol over copper-based monoliths: the effects of zirconia doping, *J. of Power Sources* 106,264-273.

Patankar S.V. (1980), *Numerical Heat Transfer and Fluid Flow*, Series in Comp. Meth. in Mech. and Therm. Sci., McGraw-Hill.

Peppley B.A., J.C. Amphlett, L.M. Kearns, R.F. Mann (1991a), Methanol-steam reforming on Cu/ZnO/AL2O3. Part 1: the reaction network, *Appl. Catal. A: Gen.* 179,21-29.

Peppley B.A., J.C. Amphlett, L.M. Kearns, R.F. Mann (1991b), Methanol-steam reforming on Cu/ZnO/AL2O3 catalysts. Part 2: A comprehensive kinetic model, *Appl. Catal. A: Gen* 179,31-49.

Purnama H., F. Girgsdies, T. Ressler, J.H. Schattka, R.A. Caruso, R. Schomäcker, R. Schlögl (2004a), Activity and selectivity of a nanostructured CuO/ZrO2 catalyst in the steam reforming of methanol, *Catal. Lett*. 94 Nos 1-2.

Purnama H., T. Ressler, R.E. Jentoft, H. Soerijanto, R. Schlögl, R. Schomäcker (2004b), CO formation/selectivity for steam reforming of methanol with a commercial CuO/ZnO/Al2O3 catalyst, *Appl. Catal. A: Gen.* 259,83-94.

Ranganathan E.S. , S.K. Bej, L.T. Thompson (2005), A methanol steam reforming over Pd/ZnO and Pd/CeO2 catalysts, *Appl. Catal.* 289,153-162.

Takeguchi T., Y. Kni, M. Inoue, K. Eguchi (2002), Steam reforming of methanol on copper catalysts supported on large-surface-area ZnAl2O3, *Catal. Lett.* 83 Nos 1-2.

Takezawa N. and N. Iwasa (1997), Steam reforming and dehydrogenation of methanol: difference in the catalytic functions of copper and group VIII metals, *Catal. Today* 36,45-56.

Zhao T. , K-D. Krever, T. Van-Nguyen (2007), *Advances in Fuel Cells*, Elsevier Ltd